

Extending the Eigenvector 1 space to the optical variability of quasars *

Yu-Feng Mao^{1,2}, Jing Wang¹ and Jian-Yan Wei¹

¹ National Astronomical Observatories, Chinese Academy of Sciences, Beijing 100012, China;
myf@bao.ac.cn

² Graduate University of Chinese Academy of Sciences, Beijing, 100049, China

Received 2008 July 1; accepted 2009 January 7

Abstract We introduce a new physical parameter, the optical variability amplitude, to the well-established Eigenvector 1 space of quasars and test a sample of long-term B-band light curves of 42 Palomar-Green quasars monitored by Giveon et al. We find that the optical variability amplitude strongly correlates with the intensity ratio of FeII to H β , H β width and peak luminosity at 5007 Å. We briefly discuss the physical meaning of our findings and suggest that the Eddington ratio may be a key factor in determining a quasar's variability.

Key words: galaxies: active — quasars: general

1 INTRODUCTION

During the last few decades, quasars have been monitored in multi-wavelength observations, from radio to X-rays, by many research programs. Our understanding of the central engine of quasars has been greatly improved by the correlations found between the variability properties and other observational parameters (e.g., luminosity, redshift, rest-wavelength, timescales and emission-line width). An anti-correlation between the amplitude of variability and luminosity was reported by Pica & Smith (1983), and confirmed by many subsequent studies (e.g., Cristiani et al. 1990; Hook et al. 1994; Cristiani et al. 1997; Giveon et al. 1999 (hereafter G99); Garcia et al. 1999; Vanden Berk et al. 2004), although there have also been reports to the contrary (e.g., Trevese et al. 1989; Giallongo et al. 1991; Cimatti et al. 1993). The relationship between the variability amplitude and redshift was discussed in many studies. Some authors found that the variability amplitude is anti-correlated with redshift (e.g., Barbieri et al. 1983; Cristiani et al. 1990; Hook et al. 1994; Cristiani et al. 1996), while others reported an opposite trend (e.g., Giallongo et al. 1991; Trevese et al. 1994; Cid Fernandes et al. 1996). Moreover, it was found that the optical spectra usually become harder as quasars turn brighter (Cutri et al. 1985; G99). Kollatschny et al. (2006) examined the variability properties of a sample of 10 Palomar-Green (PG) quasars with the line width of H β larger than 5000 km s⁻¹. They found a marginal correlation between the optical continuum variability amplitude and H β line width, which provides useful information for understanding the structure of the broad line region (BLR).

On the other hand, Boroson & Green (1992; hereafter BG92) examined a sample of 87 bright low redshift PG quasars and found that most of the variance is connected to two sets of correlations, which were then defined as Eigenvector 1 (hereafter E1) space and Eigenvector 2 space. The E1 space is

* Supported by the National Natural Science Foundation of China.

dominated by the strong anti-correlation between the optical FeII and [OIII], and Eigenvector 2 by the correlation between the optical luminosity and HeII equivalent width (see Sulentic et al. 2000a for a review). By calculating the virial black hole mass (M_{BH}) using the well established empirical $R - L$ relationship (e.g., Kaspi et al. 2000), Boroson (2002) suggested that the E1 space is dominantly driven by the Eddington ratio L/L_{Edd} , and the Eigenvector 2 by M_{BH} (see also in Sulentic et al. 2000b).

In this paper, we will investigate whether the quasars' optical variability amplitude is related to the E1 space. We test a sample of 42 PG quasars. The paper is structured as follows. The sample selection and our analysis are described in Section 2. The results are presented in Section 3, and discussions in Section 4. Throughout this paper, a Λ CDM cosmology (Spergel et al. 2003) with $\Omega_m = 0.3$, $\Omega_\Lambda = 0.7$, and $H_0 = 70 \text{ km s}^{-1} \text{ Mpc}^{-1}$ is adopted.

2 SAMPLE AND ANALYSIS

We searched the literature for suitable results of quasars' optical variability. In particular, the light curves should be well sampled in the temporal domain, with adequate total observation time and sampling interval. It is found that the G99 subset of the PG quasars is well suited for our purpose, because the optically selected PG quasars are not only nearly statistically complete but also studied comprehensively in multi-wavelength observations. G99 monitored 42 nearby ($z < 0.4$), bright ($B < 16 \text{ mag}$) PG quasars in the B and R bands for a seven-year period at Wise Observatory. The typical temporal sampling interval was 40 days and the objects were observed at 30–60 epochs with a photometry uncertainty of $\sim 0.01 \text{ mag}$. All the objects showed intrinsic rms variability amplitudes of $5\% < \sigma_B < 34\%$ and $4\% < \sigma_R < 26\%$.

Our sample is listed in Table 1. Figure 1a shows the distribution of the redshifts for the sample listed in G99, see also Col. (2) of Table 1. The redshifts of these PG quasars are mainly less than 0.2. Col. (5) lists the amplitude of variability in magnitude for each object. Furthermore, the amplitude of variability can be statistically estimated in various ways. We refer the readers to G99 for a brief comment on these different methods. In the current study, the variability is defined as the median value of all possible magnitude differences of a light curve, simply because the median value is a relatively robust estimation, i.e., not strongly affected by outliers (e.g., Hook et al. 1994; Netzer et al. 1996). Only the variability in the B band is considered in subsequent analysis since the variability is more significant in the B band than in the R band. G99 examined the correlation between the variability amplitude defined by magnitude and quasar spectral properties defining the E1. However, no significant correlations were found by them. It should be pointed out that the variability amplitude defined in magnitude represents a *relative* change in luminosity. For a constant change defined in luminosity, a small (large) change in magnitude could be simply caused if the object is (less) luminous. In order to overcome this problem, the median of absolute change in luminosity is used in this paper, that is

$$\Delta L = L_{\text{bol}} \times (1 - 10^{-0.4 \times |\text{median}(\Delta B)|}), \quad (1)$$

where $\text{median}(\Delta B)$ is the median of variability in the B band and L_{bol} the fiducial luminosity of the quasar. Note that ΔL is always positive according to this definition. ΔL represents the characteristic variability of each quasar in terms of the change in absolute luminosity, which directly reflects the absolute change in the amount of fueling gas. Regarding two quasars with the same change in the median (ΔB), the one with a larger bolometric luminosity would have a larger ΔL .

The bolometric luminosity can be estimated in two ways. First, we use a widely accepted empirical relationship

$$L_{\text{bol}} = 9\lambda L_\lambda(5100 \text{ \AA}) \quad (2)$$

as given by Kaspi et al. (2000), where the luminosities at the rest-frame wavelength 5100 \AA are adopted from Vestergaard & Peterson (2006). In another way, we also calculate the L_{bol} from the median apparent magnitudes in the B band given by G99, using the formula

$$\log(L_{\text{bol}}/v_B L_{v_B}) = 0.80 - 0.067\mathcal{L} + 0.017\mathcal{L}^2 - 0.0023\mathcal{L}^3 \quad (3)$$

Table 1 Properties of the Samples

Object (1)	z (2)	$\log(M_{\text{BH}}/M_{\odot})$ (3)	$\log(L_{\text{bol}}/L_{\text{Edd}})$ (4)	$\text{med}(\Delta B)$ (5)	$\log(\Delta L)$ (6)	FWHM(H β) (7)	Peak[OIII] (8)	RFe (9)	$\log R$ (10)
PG 0026+129	0.142	8.1	-0.1	0.16	45.1	1860	2.68	0.51	0.03
PG 0052+251	0.155	8.9	-1.1	0.22	45.0	5200	2.48	0.23	-0.62
PG 0804+761	0.100	8.5	-0.6	0.15	45.1	3070	0.46	0.67	-0.22
PG 0838+770	0.131	8.2	-0.6	0.16	44.7	2790	0.65	0.89	-0.96
PG 0844+349	0.064	7.9	-0.6	0.11	44.5	2420	0.55	0.89	-1.52
PG 0923+201	0.190	8.0	-0.1	0.18	45.0	7610	0.60	0.72	-0.85
PG 0953+414	0.239	8.7	-0.5	0.14	45.4	3130	0.84	0.25	-0.36
PG 1001+054	0.161	7.7	-0.2	0.15	44.7	1740	0.23	0.82	-0.30
PG 1012+008	0.185	8.2	-0.4	0.12	45.0	2640	1.00	0.66	-0.30
PG 1048+342	0.167	8.4	-0.8	0.27	44.7	3600	1.83	0.32	-1.00
PG 1100+772	0.313	9.3	-0.9	0.09	45.6	6160	3.99	0.21	2.52
PG 1114+445	0.144	8.6	-1.0	0.12	44.7	4570	1.36	0.20	-0.89
PG 1115+407	0.154	7.7	-0.2	0.16	44.6	1720	0.41	0.54	-0.77
PG 1121+422	0.234	8.0	-0.3	0.14	44.9	2220	2.55	0.37	-1.00
PG 1151+117	0.176	8.5	-1.0	0.16	44.8	4300	1.00	0.24	-1.15
PG 1202+281	0.165	8.6	-1.2	0.28	44.6	5050	2.27	0.29	-0.72
PG 1211+143	0.085	8.0	-0.1	0.15	45.1	1860	0.55	0.52	1.39
PG 1226+023	0.158	9.2	-0.3	0.10	46.0	3520	0.33	0.57	3.06
PG 1229+204	0.064	8.1	-0.9	0.17	44.4	3360	1.46	0.59	-0.96
PG 1307+085	0.155	8.9	-1.1	0.15	45.0	2360	2.26	0.19	-1.00
PG 1309+355	0.184	8.3	-0.5	0.09	45.0	2940	1.86	0.28	1.26
PG 1322+659	0.168	8.3	-0.5	0.08	45.0	2790	0.72	0.59	-0.92
PG 1351+640	0.087	8.8	-1.2	0.11	44.8	5660	2.27	0.24	-0.59
PG 1354+213	0.300	8.6	-0.8	0.16	45.0	4140	2.75	0.31	-1.10
PG 1402+261	0.164	7.9	-0.1	0.09	45.0	1910	0.09	1.23	-0.64
PG 1404+226	0.098	6.9	0.3	0.11	44.4	880	0.18	1.01	-0.33
PG 1411+442	0.089	8.1	-0.6	0.08	44.6	2670	0.63	0.49	-0.89
PG 1415+451	0.114	8.0	-0.6	0.07	44.6	2620	0.10	1.25	-0.77
PG 1426+015	0.086	9.1	-1.3	0.18	44.9	6820	1.47	0.39	-0.55
PG 1427+480	0.221	8.1	-0.5	0.24	44.8	2540	1.99	0.36	-0.80
PG 1444+407	0.267	8.3	-0.2	0.07	45.2	2480	0.12	1.45	-1.10
PG 1512+370	0.371	9.4	-0.9	0.13	45.6	6810	4.00	0.00	2.28
PG 1519+226	0.137	7.9	-0.4	0.10	44.7	2220	0.16	1.01	-0.05
PG 1545+210	0.266	9.3	-1.0	0.17	45.4	7030	3.66	0.00	2.62
PG 1613+658	0.129	9.2	-1.5	0.12	44.8	8450	1.99	0.38	0.00
PG 1617+175	0.114	8.8	-1.1	0.18	44.9	5330	0.48	0.60	-0.14
PG 1626+554	0.133	8.5	-1.1	0.29	44.6	4490	0.56	0.32	-0.96
PG 1700+518	0.292	8.6	-0.1	0.08	45.7	2210	0.00	1.42	0.37
PG 1704+608	0.371	9.4	-0.8	0.13	45.7	6560	6.50	0.00	2.81
PG 2130+099	0.061	7.9	-0.5	0.09	44.5	2330	0.89	0.64	-0.49
PG 2233+134	0.325	8.0	0.1	0.10	45.3	1740	0.77	0.89	-0.55
PG 2251+113	0.323	9.0	-0.5	0.06	45.7	4160	1.69	0.32	2.56

Col. (1): object Name; Col. (2): redshift; Col. (3): the logarithm of the black hole mass, as given by Vestergaard & Peterson (2006); Col. (4): the logarithm of the Eddington ratio, as given by Vestergaard & Peterson (2006); Col. (5): median(ΔB), in units of mag; Col. (6): $\log(\Delta L)$, defined as the Equation (1); Col. (7): the FWHM of the broad component of H β , in units of km s $^{-1}$; Col. (8): the peak height of [OIII]5007; Col. (9): the RFe; Col. (10): the logarithm of the radio power.

of Marconi et al. (2004), where $\mathcal{L} = (\log L_{\text{bol}} - 12)$. A comparison between the values of L_{bol} obtained from Equation (2) and those from Equation (3) is made (see Fig. 2). There is a strong correlation (with slope ~ 1) between the two sets of L_{bol} , indicating that the two independent measurements are highly consistent with each other. So, we adopt the value of L_{bol} obtained from Equation (2), and then calculate the ΔL using Equation (1). The calculated ΔL in the logarithm is shown in Col. (6) of Table 1 for each quasar.

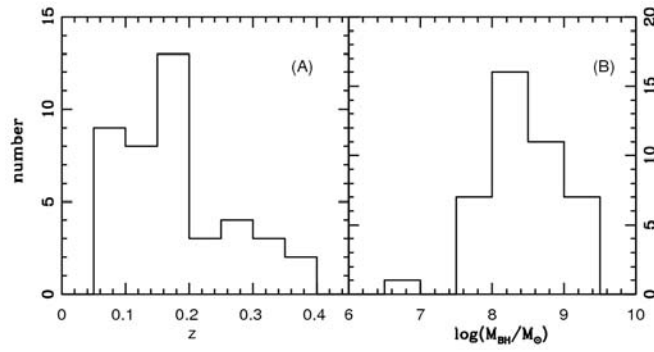


Fig. 1 Distribution of redshift (Panel A) and black hole mass (Panel B) for the 42 PG quasars studied in this paper.

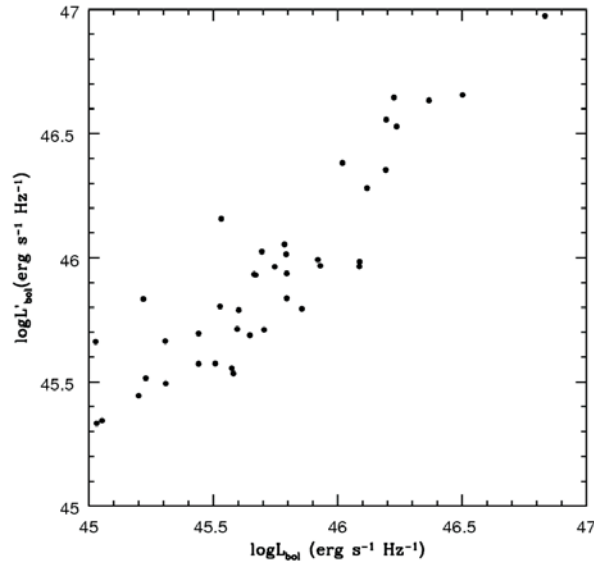


Fig. 2 Comparison between the value of L_{bol} calculated from Eqs. (2) and (3). The horizontal axis represents the L_{bol} from Eq. (2) (Kaspi et al. 2000), and the vertical axis represents the L'_{bol} from Eq. (3) (Marconi et al. 2004). It is clear that the two independent measurements are consistent with each other.

3 RESULTS

The main goal of the present paper is to investigate whether the variability amplitude of quasars is related to E1 space. The E1 space is dominated by significant correlations between RFe ($=\text{FeII}/\text{H}\beta$), FWHM($\text{H}\beta$) and [OIII] strength, which has been discussed by many authors (e.g. BG92; Xu et al. 2003; Grupe 2004; Sulentic et al. 2000a). We list the E1 parameters of our PG quasar sample in Table 1. Col. (7) gives the FWHM of the broad component of $\text{H}\beta$, Col. (8) the ratio of the peak height of [OIII] $\lambda 5007$ to that of $\text{H}\beta$ (Peak $\lambda 5007$), Col. (9) the ratio of the flux of FeII integrated in the rest frame wavelength range from $\lambda 4434$ to $\lambda 4684$ to that of $\text{H}\beta$ (RFe), Col. (10) the logarithm of R , i.e., the ratio of radio flux at 6 cm to optical flux density. All of these parameters are adopted from BG92.

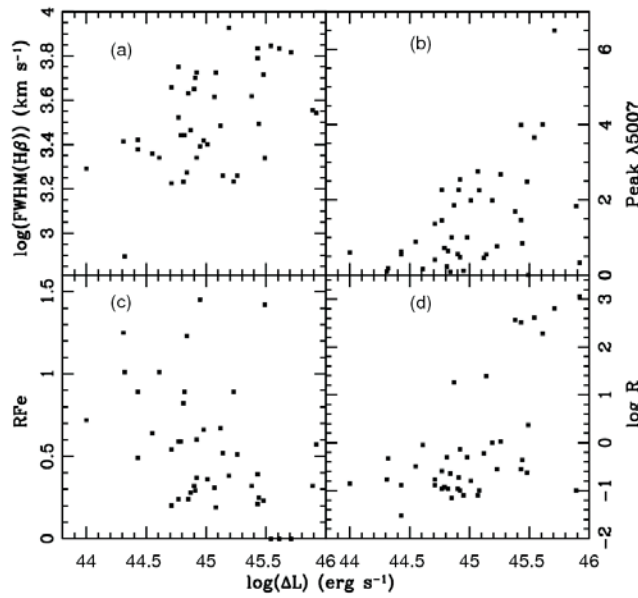


Fig. 3 Plots of ΔL vs. E1 parameters. The horizontal axis represents the ΔL , and the vertical axis represents the E1 parameters: (a) $\log(\text{FWHM}(\text{H}\beta))$ ($r_s = 0.450$, $P_s = 0.004$) (b) peak $\lambda 5007$ ($r_s = 0.445$, $P_s = 0.0044$). (c) RFeII ($r_s = -0.441$, $P_s = 0.0048$). (d) $\log R$ ($r_s = 0.476$, $P_s = 0.0023$).

Table 2 Spearman Rank-Order Correlation Coefficients of the Correlations Shown in Fig. 3

ΔL vs.	FWHM (H β)	Peak $\lambda 5007$	RFe	$\log R$
r_s	0.450	0.445	-0.441	0.476
P_s	0.004	0.004	0.005	0.002

We then investigate the correlations between the ΔL and E1 parameters in our sample. Figure 3 displays the correlations of ΔL versus FWHM(H β), peak $\lambda 5007$, RFe, and the radio loudness $\log R$, respectively. The spearman rank-ordered correlation coefficients r_s of the four correlations are listed in Table 2, where P_s is the probability of null correlation. Figure 3a shows a significant correlation between the ΔL and FWHM(H β). A spearman rank-ordered analysis yields a correlation coefficient $r_s=0.450$ with a significance level $P_s=0.004$. This means that the quasars with widths larger than H β would have larger changes in luminosity. We also find a correlation between ΔL and peak $\lambda 5007$ (Fig. 3b, $r_s = 0.445$, $P_s = 0.004$). The anti-correlation between ΔL and RFe is plotted in Figure 3c. The calculated correlation coefficient is $r_s = -0.441$, and the significance level $P_s = 0.005$. Kollatschny et al. (2006) did not find a significant correlation between the continuum variability amplitude at 5100 Å and radio power at 5 GHz in their sample. In current studies, a correlation ($r_s = 0.476$, $P_s = 0.0023$) is identified between the radio loudness $\log R$ and ΔL , and is shown in Figure 3d. Since $\log R = 1$ is widely used to separate the radio-loud and radio-quiet quasars (Kellermann et al. 1989), the diagram shows that all the radio-loud quasars ($\log R > 1$) have large optical variability amplitudes ($\log(\Delta L) > 45$), although the radio-quiet quasars ($\log R < 1$) are nearly evenly distributed in terms of variability amplitude. The fact that radio-loud quasars have large variability amplitudes implies that the optical continuum of radio-loud quasars is contaminated by the high energy tails of their radio emissions, which boosts the variability amplitude because of the beam effect of the jets.

Table 3 Correlations of Eigenvectors with Line and Continuum Properties

Property	Eigenvector 1	Eigenvector 2	Eigenvector 3	Eigenvector 4
Eigenvalue	3.89	1.87	1.24	1.03
Cumulative (%)	35.3	52.3	63.6	73.0
$\log R$	0.68	0.54	-0.15	0.03
EW($H\beta_b$)	-0.05	-0.60	-0.55	-0.08
$R(\lambda 5007)$	0.82	0.04	0.43	-0.13
$R(\lambda 4686)$	-0.14	-0.55	0.44	-0.23
RFe	-0.79	0.45	-0.03	-0.04
Peak ($\lambda 5007$)	0.92	-0.07	0.24	-0.12
FWHM($H\beta_b$)	0.68	-0.21	-0.32	0.34
$H\beta$ shift	-0.10	0.39	0.46	0.05
$H\beta$ shape	0.07	0.27	-0.29	-0.89
$H\beta$ asymm	-0.70	-0.33	0.02	0.15
$\log(\Delta L)$	0.54	0.57	-0.30	0.10

The correlations found above suggest that the E1 space could be extended to include the variability amplitude. This hypothesis can be verified by a principal component analysis (PCA) of our sample. The PCA is performed using the following 11 parameters: $\log R$, the equivalent width of $H\beta$, $R(\lambda 5007)$, $R(\lambda 4686)$, RFe, Peak($\lambda 5007$), FWHM($H\beta$), $H\beta$ shift, $H\beta$ shape, $H\beta$ asymmetry, and $\log(\Delta L)$, with each potentially providing unique information. Except for $\log(\Delta L)$, the former ten parameters are directly collected from BG92. We refer the reader to BG92 for the definitions of these parameters. The PCA results are presented in Table 3, which lists the first four most significant eigenvectors. The second row shows the cumulative percentage of the variance. One can see that the first four eigenvectors together account for more than 70 percent of the variance, and that the first principal component dominates the observed properties of quasars. Similar to BG92, the E1 is dominated by the anti-correlation between the strength of FeII and Peak ($\lambda 5007$). In addition, our E1 is strongly affected by $\log(\Delta L)$. It is clear that $\log(\Delta L)$ has a projection of 0.54 on E1, and 0.57 on E2. Although at first sight, the projection on Eigenvector 2 is larger than on E1, taking the larger cumulative percentage of E1 into account, we conclude that the E1 space can be extended to $\log(\Delta L)$.

4 DISCUSSION

4.1 Variability vs. M_{BH} and Eddington Ratio

After extending the E1 space to the variability in amplitude, the dominant physical parameters are discussed in this section. Both the black hole mass (M_{BH}) and Eddington ratio (L/L_{Edd}) are believed to be the main parameters governing the observed properties in quasars. However, the luminosity variability defined by Equation (1) cannot be used to correlate with M_{BH} and L/L_{Edd} because both M_{BH} and L/L_{Edd} are estimated in terms of the continuum luminosity which is used to define the variability in luminosity. The variability in median magnitude (ΔB) is therefore used instead in the subsequent analysis. All M_{BH} values are adopted from Vestergaard & Peterson (2006). The distribution of M_{BH} is shown in Figure 1b. One can see that the majority of $\log(M_{\text{BH}}/M_{\odot})$ lie between 7.5 and 9.5. L_{bol} is then estimated using the Equation (2). The values of M_{BH} and L/L_{Edd} are listed in Cols. (3) and (4) in Table 1, respectively.

The relation between the variability amplitude and M_{BH} or L/L_{Edd} has been discussed recently. Contradictory results were, however, obtained by different authors. Wold et al. (2007) examined the relation between the quasar variability and black hole mass by studying the optical variability of ~ 100 quasars monitored by the QUEST1 survey (Rengstorff et al. 2004). However, a correlation between the R-band variability and M_{BH} was marginally obtained only when M_{BH} was averaged in several bins. Furthermore, they did not detect such a relation in their PG quasar sample. In contrast, Wilhite et al. (2008) found a correlation between the variability and M_{BH} in a sample of ~ 2500 quasars selected from the SDSS. In addition, they reproduced the well-known anti-correlation between the variability

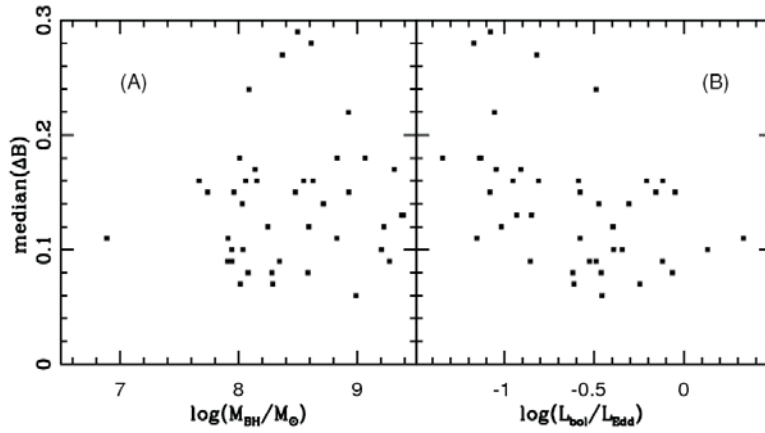


Fig. 4 Panel A: median magnitude change vs. black hole mass ($r_s = 0.124$, $P_s = 0.4267$). Panel B: median magnitude change vs. Eddington ratio ($r_s = -0.368$, $P_s = 0.0012$).

and luminosity. By combining the two relations, they suspected that L/L_{Edd} is a possible driver for quasar variability in an indirect way.

As $M_{\text{BH}} \propto (\text{FWHM})^2$, a possible way to test the correlation between variability and M_{BH} is to search for the correlation between the variability and line width, both of which are independent observational parameters. The relation between the variability amplitude and line width was discussed in several papers. G99 found a marginal correlation between the variability amplitude (defined in magnitude) and width of the $\text{H}\beta$ emission line. Their possible, but unlikely explanation, for this trend is the contributions of the emission lines to the broad-band emission. Kollatschny et al. (2006) confirmed the results of G99 in a sample of 43 galaxies. In the above analysis, we find a significant correlation between $\log(\Delta L)$ and the FWHM of $\text{H}\beta$ (Fig. 3a).

The median (ΔB) is plotted against M_{BH} in Figure 4a. No significant correlation is, however, found between these two parameters ($r_s = 0.124$, $P_s = 0.4267$). Wold et al. (2007) did not detect a correlation between variability and M_{BH} in their PG quasar sub-sample, and our result confirms their conclusion. However, the current results make it difficult to understand why the correlation between the magnitude variability and the M_{BH} is not as good as expected.

It is now generally believed that the E1 space is likely driven by L/L_{Edd} (e.g., Boroson 2002). The relation between the magnitude variability and L/L_{Edd} is directly examined in Figure 4b. We find a significant anti-correlation between the median (ΔB) and L/L_{Edd} ($r_s = -0.368$, $P_s = 0.0012$). Although our result agrees with Wilhite et al. (2008), caution must be made when explaining the median (ΔB)- L/L_{Edd} correlation. Taking two quasars with the same M_{BH} , the more luminous one would have smaller variability in magnitude for a given change in luminosity (accretion rate). Meanwhile, the more luminous quasar would have a larger L/L_{Edd} . That means that the median (ΔB)- L/L_{Edd} correlation might be caused by an intrinsic relation in mathematics (i.e., the definition of magnitude) rather than in physics. A sample of light curves defined in flux or luminosity is therefore required to test the underlying physics of the relation.

4.2 Implications on Variability Mechanisms

Several theoretical models have been proposed as mechanisms for variability in quasars, such as disk-instability (Kawaguchi et al. 1998), gravitational microlensing (Hawkins 1993, 1996), and starburst (Terlevich et al. 1992). However, all of these are still far from being clear.

Hawkins (1993, 1996) explained the observed AGN variability by invoking gravitational microlensing. In this model, a quasar's light is lensed by a large population of compact bodies with planetary-mass. The microlensing model has two parameters: the Einstein radius of the lenses and their mean transverse velocity (Hawkins 2002). However, the two parameters generally cannot be obtained observationally. In addition, microlensing events should be extremely rare at low redshift (Vanden Berk et al. 2004). This explanation can be easily excluded for the PG quasars studied in this paper. We find the quasar's variability is related to the E1 space, which strongly indicates that the variability must be caused by an intrinsic mechanism rather than an external one.

Some researchers endorse the idea that AGN variability might be caused by a series of discrete outbursts, such as supernova explosions (Aretxaga et al. 1997). However, this model cannot explain the relationship between the luminosity and variability amplitude as argued by Pica & Smith (1983). Alternatively, Terlevich et al. (1992) explained the AGN variability as originating from the supernova remnants (SNRs) which occurs in the innermost regions of AGNs. The long-term and short-term variability observed in AGNs could be explained by the long-term decay of the SNRs and cooling instability after the onset of the radiative phase, respectively. The cooling time before the radiative phase is ~ 0.6 yr, and beyond this, the phase is reduced to ~ 6 d.

The disk-instability model is much more popular than the other models. This model interprets the variability as an occasional flare event or blob formation caused by the instability in the accretion disk. Kawaguchi et al. (1998) compared the logarithmic slopes of the structure function between the disk-instability model and star-burst model, and their observation of quasar 0957+561 supports the disk-instability model. Vanden Berk et al. (2004) studied photometric variability of 25000 quasars from SDSS, and found that their results favor the disk-instability model. However, it is still unclear how changes in the accretion rate or the resulting luminosity changes would propagate through the accretion disk. Recently, Li & Cao (2008) proposed a disk model, and suggested that the disk temperature change would lead to systematic differences in spectral shape, which could explain the correlation between the variability and L/L_{Edd} or M_{BH} discovered by Wold et al. (2007) and Wilhite et al. (2008).

Although our analysis cannot discriminate which model, starburst or disk-instability is favored for a quasar's variability, the extension of the E1 space to the variability implies that either: 1) the stability of the accretion rate (or gas supply) changes along the E1 sequence in the disk-instability model, or 2) the intensity of star formation activity changes along the E1 sequence.

5 CONCLUSIONS

By studying the variability of the 42 PG quasars monitored by Giveon et al. (1999), using both direct correlations and PCA analysis, we find that the E1 space can be extended to include quasars' optical variability. The link between this variability and Eddington ratio/black hole mass is discussed, and we propose that the Eddington ratio may be a key factor in determining the variability of quasars.

Acknowledgements We would like to thank the anonymous referee for constructive comments that improved the paper. We also thank Prof. J. M. Wang, Drs. W. H. Bian, D. W. Xu, J. S. Deng and James Wicker for valuable discussion and help. This work was supported by the National Science Foundation of China (Nos. 10803008 and 10873017) and National Basic Research Program of China.

References

- Aretxaga, I., Cid Fernandes, R., & Terlevich, R. J. 1997, MNRAS, 286, 271
- Barbieri, C., Cristiani, S., Nardon, G., & Romano, G. 1983, LIACo, 24, 443
- Boroson, T. A., & Green, R. F. 1992, ApJS, 80, 109
- Boroson, T. A. 2002, ApJ, 565, 78
- Cid Fernandes, R., Aretxaga, I., & Terlevich, R. 1996, MNRAS, 282, 1191
- Cimatti, A., Zamorani, G., Marano, B. 1993, MNRAS, 263, 236
- Cristiani, S., Vio, R., & Andreani, P. 1990, AJ, 100, 56

- Cristiani, S., Trentini, S., La Franca, F., Aretxaga, I., Andreani, P., Vio, R., & Gemmo, A. 1996, *A&A*, 306, 395
- Cristiani, S., Trentini, S., La Franca, F., & Andreani, P. 1997, *A&A*, 321, 123
- Cutri, R. M., Wisniewski, W. Z., Rieke, G. H., & Lebofsky, M. J. 1985, *ApJ*, 296, 423
- Garcia, A., Sodre, L. J., Jablonski, F. J., & Terlevich, R. J. 1999, *MNRAS*, 309, 803
- Giallongo, E., Trevese, D., & Vagnetti, F. 1991, *ApJ*, 377, 345
- Giveon, U., Maoz, D., Kaspi, S., Netzer, H., & Smith, P. S. 1999, *MNRAS*, 306, 637
- Grupe, D. 2004, *AJ*, 127, 1799
- Hawkins, M. R. S. 1993, *Nature*, 366, 242
- Hawkins, M. R. S. 1996, *MNRAS*, 278, 787
- Hawkins, M. R. S. 2002, *MNRAS*, 329, 76
- Hook, I. M., McMahon, R. G., Boyle, B. J., & Irwin, M. J. 1994, *MNRAS*, 268, 305
- Kaspi, S., et al. 2000, *ApJ*, 533, 631
- Kawaguchi, T., Mineshige, S., Umemura, M., & Turner, E. L. 1998, *ApJ*, 504, 671
- Kellermann, K. I., Sramek, R., Schmidt, M., et al. 1989, *AJ*, 98, 1195
- Kollatschny, W., Zetzl, M., & Dietrich, M. 2006, *A&A*, 454, 459
- Li, S., & Cao, X. 2008, *MNRAS*, 387, L41
- Marconi, A., Risaliti, G., & Gilli, G., et al. 2004, *MNRAS*, 351, 169
- Netzer, H., Heller, A., Loinger, F., et al. 1996, *MNRAS*, 279, 429
- Pica, A. J., & Smith, A. G. 1983, *ApJ*, 272, 11
- Rengstorf, A. W., Mufson, S. L., et al. 2004, *ApJ*, 606, 741
- Spergel, D. N., Verde, L., Peiris, H. V., et al. 2003, *ApJS*, 148, 175
- Sulentic, J. W., Marziani, P., & Dultzin-Hacyan, D. 2000a, *ARA&A*, 38, 521
- Sulentic, J. W., Zwitter, T., Marziani, P., & Dultzin-Hacyan, D. 2000b, *ApJ*, 536, L5
- Terlevich, R., Tenorio-Tagle, G., Franco, J., & Melnick, J. 1992, *MNRAS*, 255, 713
- Trevese, D., Pittella, G., Kron, R. G., Koo, D. C., & Bershadsky, M. 1989, *AJ*, 98, 108
- Trevese, D., Kron, R. G., Majewski, S. R., Bershadsky, M., & Koo, D. C. 1994, *ApJ*, 433, 494
- Vanden Berk, D. E., Wilhite, B. C., Kron, R. G., et al. 2004, *ApJ*, 601, 692
- Vestergaard, M., & Peterson, B. 2006, *ApJ*, 641, 689
- Wilhite, B. C., Brunner, R. J., Grier, C. J., et al. 2008, *MNRAS*, 383, 1232
- Wold, M., Brotherton, M. S., & Shang, Z. 2007, *MNRAS*, 375, 989
- Xu, D. W., Komossa, S., Wei, J. Y., Qian, Y., & Zheng, X. Z. 2003, *ApJ*, 590, 73